

## A Critical Analysis of the Relaxation Rates for Device Modeling

Tilmann Kuhn, Lino Reggiani, Luca Varani

*Dipartimento di Fisica e Centro Interuniversitario di Struttura della Materia  
 dell'Università di Modena, Via Campi 213/A, 41100 Modena, Italy*

*Phone: +39-59-586045, Fax: +39-59-367488*

### Abstract

This communication presents a critical analysis of the relaxation rates which are used in the hydrodynamic models for the simulation of semiconductor devices. From the balance equations and the correlation functions for a set of relevant variables we show that at least three different definitions of relaxation rates can be introduced. The results so obtained for the case of p-type Si at 77 K are discussed in terms of similarities, differences, and corresponding ranges of application.

### 1 Introduction

The modeling of semiconductor devices by using hydrodynamic equations requires the knowledge of a set of phenomenological relaxation rates which are connected with the corresponding hydrodynamic variables velocity  $\mathbf{v}$  and energy  $\varepsilon$  of the carriers [1,2,3,4]. At low temperatures, when the dopants are only partially ionized, the fraction of free carriers  $u$  becomes field-dependent and thus also becomes a hydrodynamic variable. Then, from the balance equations [5,6], for the case of homogeneous and steady-state conditions at the given field, the corresponding phenomenological rates are introduced:

$$\tau_u^{-1} = \frac{1}{\langle u \rangle \tau_g} \quad (1)$$

$$\tau_{v_l}^{-1} = \frac{eE}{m \langle v_l \rangle} \quad (2)$$

$$\tau_\varepsilon^{-1} = \frac{e \langle v_l \rangle E}{\langle \varepsilon \rangle - \frac{3}{2} K_B T} \quad (3)$$

where  $1/\tau_u$  is the number (carrier density) relaxation rate,  $1/\tau_{v_l}$  the longitudinal velocity relaxation rate, and  $1/\tau_\varepsilon$  the energy relaxation rate. In the above equations  $\tau_g$  is the mean generation time,  $m$  is the effective mass (here assumed energy independent),  $e$  the electronic charge,  $v_l$  the longitudinal velocity,  $E$  the electric field,  $K_B$  the Boltzmann constant,  $T$  the lattice temperature and brackets indicate ensemble averages. However, these rates in general do not describe rigorously the relaxation of the variables to their stationary value. Due to microscopic coupling between different variables, this relaxation is related to a relaxation matrix which describes the time decay of the correlation functions of the corresponding variables. In the following we will show that the knowledge of this matrix and its eigenvalues represents a useful tool for the physical analysis of different relaxation processes. Therefore, the scope of this work is to present

the different definitions of relaxation rates, discussing the main similarities and discrepancies among them and the corresponding ranges of application.

## 2 Theory

Starting from a quantum mechanical derivation of generalized Langevin equations, it has been shown [7] that under suitable approximations (i.e. separation of the time-scales between the "relevant" and the "irrelevant" variables and neglect of memory effects) a closed system of equations of motion for the correlation functions of a complete set of relevant variables  $P_m$ ,  $m = 1, \dots, M$  can be obtained in the form of a set of coupled relaxation equations as:

$$\frac{d}{dt}\Phi_{ij}(t) = -\sum_{k=1}^M \alpha_{jk}\Phi_{ik}(t) \quad (4)$$

where

$$\Phi_{ij}(t) = \langle \delta P_i(0)\delta P_j(t) \rangle \quad (5)$$

with  $\delta P_i(t) = P_i(t) - \langle P_i \rangle$ . The important property of Eq. (4) is the fact that the relaxation matrix  $\alpha$  does not depend on the index  $i$  of the first variable. This permits a unique determination of the elements  $\alpha_{ij}$  from the knowledge of the initial conditions  $\Phi_{ij}(0)$  and  $\frac{d}{dt}\Phi_{ij}(0)$ . The elements are given by the standard formula:

$$\alpha_{ij} = \frac{D_{ij}}{D} \quad (6)$$

where  $D = \det\{\Phi_{kl}(0)\}$  and  $D_{ij}$  is the determinant obtained from  $D$ , if in column  $j$  the values  $\Phi_{kj}(0)$  are replaced by  $-\frac{d}{dt}\Phi_{ki}(0)$ . The general solution of Eq. (4) can be written as

$$\Phi_{ij}(t) = \sum_{\nu=1}^M c_i^{(\nu)} \psi_j^{(\nu)} e^{-\alpha^{(\nu)}t} \quad (7)$$

where  $\alpha^{(\nu)}$  is the  $\nu$ -th eigenvalue of  $\alpha$ ,  $\psi_j^{(\nu)}$  the  $j$ -th component of the corresponding eigenvector and  $c_i^{(\nu)}$  the expansion coefficient given by the scalar product

$$c_i^{(\nu)} = \sum_{k=1}^M \Phi_{ik}(0) \tilde{\psi}_k^{(\nu)}. \quad (8)$$

$\tilde{\psi}_k^{(\nu)}$  is the eigenvector of the transposed matrix  $\alpha^T$  corresponding to the eigenvalue  $\alpha^{(\nu)}$  and we have taken normalized eigenvectors. The relaxation matrix  $\alpha$  in general is not symmetric, thus, the eigenvalues may not only be real, but there can also exist pairs of complex conjugate values. Since the correlation functions must be real, in this case also the eigenvectors and expansion coefficients must be complex conjugate.

Within the above scheme we are now able to analyze the various correlation functions and the corresponding relaxation rates.

### 3 Results

As application we have used a Monte Carlo (MC) simulation to calculate first-order and second-order quantities of the relevant variables for the case of charge transport in nondegenerate p-type Si at 77 K under the influence of an electric field of arbitrary strength. We consider the strong extrinsic regime (i.e. negligible compensation) with a two level conduction mechanism, the impurity centers and the conducting band. The microscopic model uses a single valence band (the heavy hole band) warped with nonparabolicity effects accounted for. Acoustic, nonpolar optical, ionized impurity scattering, and impact ionization from shallow centers are included in the simulation. A nonradiative generation-recombination (GR) mechanism from shallow levels assisted by acoustic phonon (cascade capture model) is introduced. A linear recombination kinetics is considered and the Poole-Frenkel effect is accounted for [8]. The very good agreement obtained between calculations and experiments, which supports the physical reliability of the model used, have been already reported in Ref. [9].

Figure 1 shows the mean values of the fraction of free carrier, the longitudinal velocity, and the carrier energy as a function of the electric field.

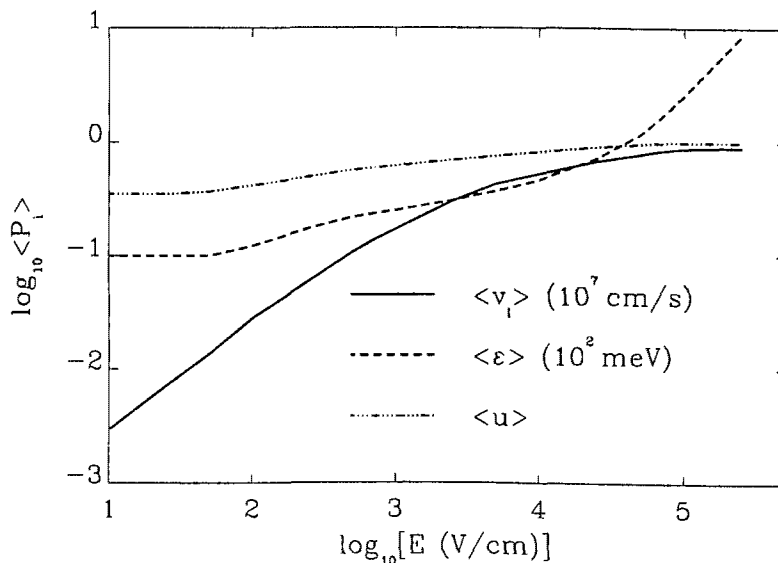


Figure 1: Mean values of the relevant variables as a function of the electric field applied parallel to the  $\langle 100 \rangle$  crystallographic direction. Values are obtained from a Monte Carlo simulation for the case of p-type Si at 77 K with an acceptor concentration  $N_A = 3 \times 10^{15} \text{ cm}^{-3}$ .

Since we have a cubic semiconductor with an electric field in the  $\langle 100 \rangle$  direction, the mean value of the transverse velocity remains always zero. The fraction of free carriers increases with increasing field mostly due to the suppression of recombination processes which occur practically only from the bottom of the band. At high fields the generation mechanism is additionally enhanced due to the Poole-Frenkel effect and eventually  $u$  reaches unity because there all impurities are ionized. The longitudinal average velocity, after an initial Ohmic increase, tends to saturate at fields above some  $10 \text{ kV/cm}$ . The mean energy at intermediate fields shows only a slight increase and at high fields, when the cooling due to optical phonons becomes less efficient, increases strongly.

From the results concerning the correlation functions, it emerges that the five variables  $u$ ,  $\mathbf{v}$

and  $\varepsilon$  to a good approximation indeed form a complete set of relevant variables. For symmetry reasons the transverse velocities  $v_t$  do not couple to the other three variables. Thus, the matrix  $\alpha$  is diagonal with respect to these quantities, the diagonal elements being identical and defining the relaxation rate of the transverse velocity. Effectively, we have to consider only a  $3 \times 3$  matrix for the variables  $u$ ,  $v_t$  and  $\varepsilon$ . Although in Ref. [7] the microscopic formula for the matrix  $\alpha$  is derived using projection operators into the relevant subspace, for any real bandstructure and interaction processes this formula is impossible to be solved analytically. However, at a phenomenological level,  $\alpha$  is totally determined by Eq. (6). Thus, using the initial values  $\Phi_{ij}(0)$  and  $\frac{d}{dt}\Phi_{ij}(0)$  from the MC simulation as input, we can calculate the matrix  $\alpha$ , its eigenvalues and eigenvectors as well as the expansion of  $\Phi_{ij}(t)$  into the sum of the exponential functions in Eq. (7).

Figure 2 shows the auto-correlation functions and Fig. 3 the cross-correlation functions for an intermediate field strength.

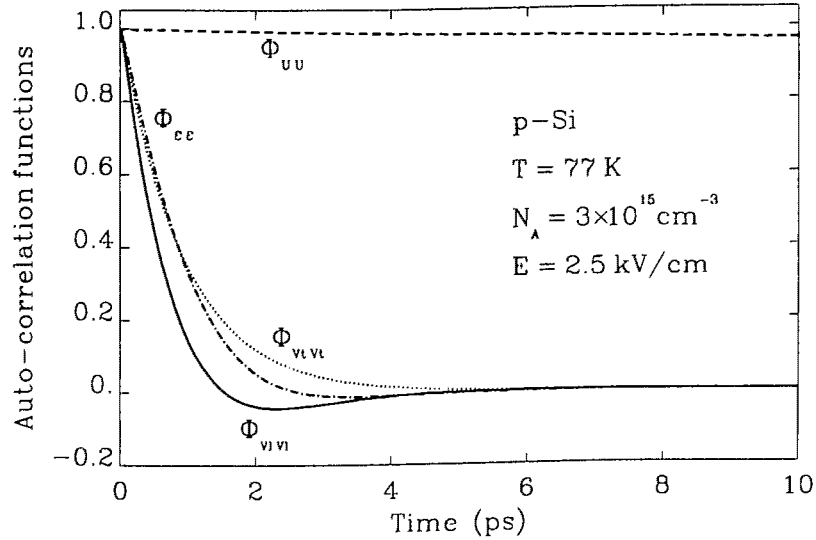


Figure 2: Auto-correlation functions normalized to their initial values in p-Si at 77 K with  $N_A = 3 \times 10^{15} \text{ cm}^{-3}$  at an electric field of 2.5 kV/cm as a function of time obtained from the expansion into eigenvectors of the matrix  $\alpha$ .

By using the property  $\langle \delta P_i(0) \delta P_j(t) \rangle = \langle \delta P_i(-t) \delta P_j(0) \rangle$ , we have drawn the cross-correlation functions on a symmetric time axis so that each curve corresponds to a pair of functions. Here, because of the far from equilibrium conditions, all correlation functions exhibit structures which are related to the different scales of the relaxation rates involved. The shape of the auto-correlation functions has already been discussed in the literature [10]. Therefore, we concentrate on the cross-correlation functions which have been only recently presented by the authors [11]. Due to the symmetry all cross-correlations with the transverse velocity vanish. The structure of the other cross-correlation functions is related to the energy dependence of the scattering mechanisms, which in the present case always leads to an increase of the scattering rate with increasing energy. Therefore, when considering the correlation function between  $v_t$  and  $\varepsilon$ , we argue as follows: In the positive time region, if initially a positive fluctuation of  $v_t$  occurs, at a later time, due to the large absorbed power, a positive fluctuation of  $\varepsilon$  is likely to occur; for the same reason an initial negative fluctuation of  $v_t$  will lead to a negative fluctuation of  $\varepsilon$ .

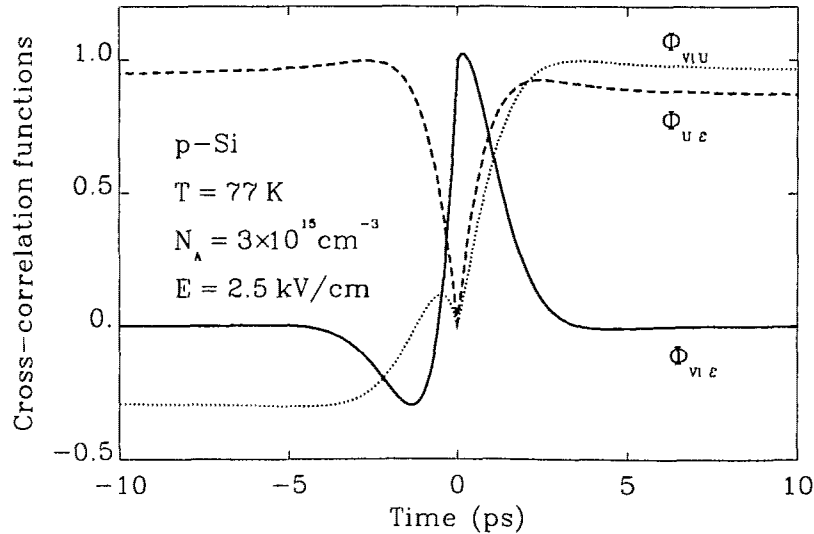


Figure 3: Cross-correlation functions in p-Si at 77 K with  $N_A = 3 \times 10^{15} \text{ cm}^{-3}$  at an electric field of 2.5 kV/cm as a function of time obtained from the expansion into eigenvectors of the matrix  $\alpha$ . Continuous, dotted, and dashed lines refer, respectively, to  $\Phi_{v_i \epsilon}(t)$ ,  $\Phi_{v_i u}(t)$  and  $\Phi_{u \epsilon}(t)$ . The function  $\Phi_{v_i \epsilon}(t)$  is normalized to its initial value, other functions, having a zero initial value, are normalized to their maximum.

Thus, the initial slope of the correlation function between  $v_i$  and  $\epsilon$  will always be positive. On the other hand, in the negative time region, we find that if initially a positive fluctuation of  $\epsilon$  occurs, at a later time, due to the increased efficiency of the scattering, a negative fluctuation of  $v_i$  is likely to occur; for the same reason an initial negative fluctuation of  $\epsilon$  will lead to a positive fluctuation of  $v_i$ . Thus, the initial slope of the correlation function between  $\epsilon$  and  $v_i$  will always be negative. At short times its behavior is governed by the relaxation time of the longitudinal velocity, while the asymptotic decrease is governed by the energy relaxation-time. This function vanishes linearly at lowering field strengths.

The cross-correlation functions between the fraction of free carriers and energy or velocity vanish at zero time because in the case of non-interacting particles these fluctuations are independent. Due to the energy dependence of the recombination and generation probability, however, fluctuations at different times are correlated. An initial positive fluctuation of  $u$  leads to an increase in the recombination probability near the bottom of the band, thus increasing the average energy of the carriers in the band. Also, an initial negative fluctuation of  $u$  leads to a large generation probability at low energies reducing the average energy of the carriers. Therefore, the correlation between  $u$  and  $\epsilon$  increases on the time-scale of the energy relaxation time and then returns to zero on the time-scale of the lifetime. In the negative time region the function exhibits qualitatively the same structure, since an initial positive (negative) fluctuation in energy leads to a decrease (increase) in the recombination probability. Thus, it is likely to have a positive (negative) fluctuation in  $u$  at later times. The correlation function between  $v_i$  and  $u$  has the most complicated structure. In the positive time region its behavior is qualitatively like that one of the correlation function between  $\epsilon$  and  $u$ . Since GR processes are symmetric in  $k$ -space, the time-dependence is mainly governed by the energy fluctuation which is always associated with an initial velocity fluctuation. In the negative time region, however,

all three characteristic time-scales are important. The reason for this is the following: As already discussed above, a positive fluctuation in  $u$  leads to an increase in recombination from the bottom of the band. Since particles with a small velocity are removed, the average velocity increases. But now also the average energy of the carriers increases leading to a stronger scattering efficiency (see the discussion for the correlation function between  $v_l$  and  $\varepsilon$ ). Therefore, the velocity decreases below its mean value and the correlation function becomes negative. Finally, on the time-scale of the lifetime, the system returns to its stationary state and the correlations disappear. The same arguments hold for the time-evolution after an initial negative fluctuation in  $u$ .

In Figure 4 we have plotted the phenomenological relaxation rates of Eqs. (1) to (3).

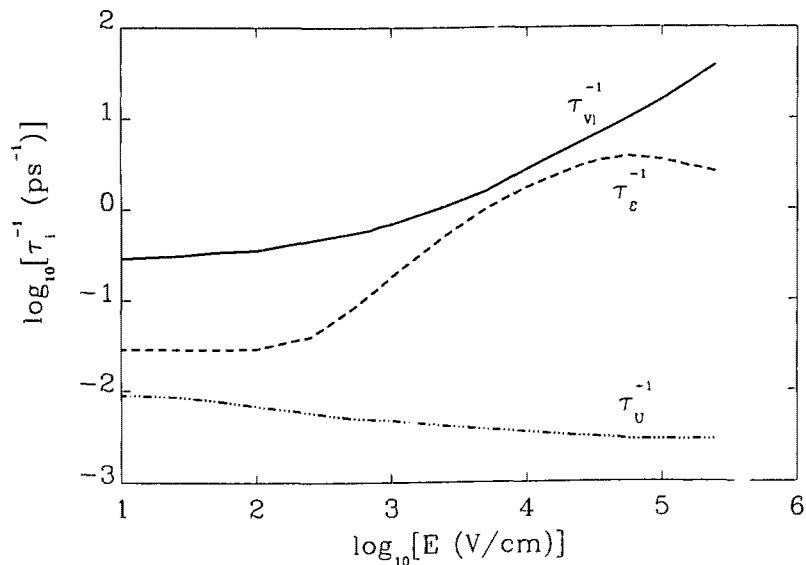


Figure 4: Phenomenological relaxation rates as a function of the electric field applied parallel to the  $\langle 100 \rangle$  crystallographic direction. Values are obtained from the Monte Carlo simulation for the case of p-type Si at 77 K with  $N_A = 3 \times 10^{15} \text{ cm}^{-3}$ .

Their field dependence reflects the presence of hot-electron conditions. Accordingly, at increasing fields the number relaxation rate tends to decrease because of the field assisted ionization mechanism which is due to both: carrier heating and Poole-Frenkel effect. The longitudinal-velocity relaxation rate tends to increase because of the increased efficiency of the scattering mechanisms. The energy relaxation rate exhibits a maximum at about  $50 \text{ kV/cm}$  and then decreases at the highest fields because of the smaller efficiency of scattering to dissipate the excess energy gained by the field.

Figure 5 shows the field dependence of the diagonal components of the relaxation matrix, calculated from the correlation functions as given by Eq. (6) (in this case, also the transverse velocity relaxation rate can be evaluated).

In the absence of coupling they would represent the respective relaxation rates for the fraction of free carriers, their velocity and energy. Indeed, their field dependence is in good agreement with the phenomenological rates of Fig. 4.

In order to interpret the coupling in the relaxation processes, we have calculated the eigenvalues of the relaxation matrix  $\alpha$  as a function of the electric field and we have plotted them in Fig. 6.

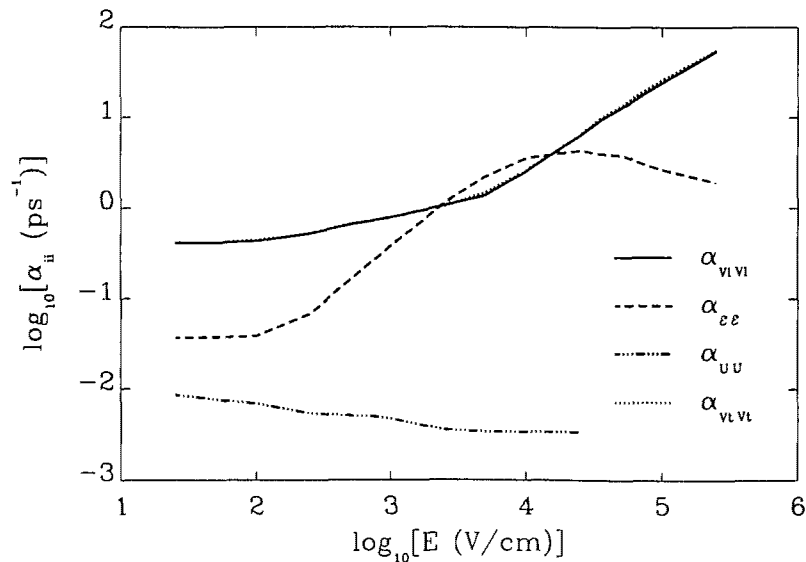


Figure 5: Diagonal elements of the relaxation matrix  $\alpha$  as a function of the electric field applied parallel to the  $\langle 100 \rangle$  crystallographic direction. Values are obtained from the Monte Carlo simulation for the case of p-type Si at 77 K with  $N_A = 3 \times 10^{15} \text{ cm}^{-3}$ .

At low electric fields we have three different real decay rates, they can be interpreted as number relaxation rate, velocity relaxation rate and energy relaxation rate. Due to the cubic symmetry, at vanishing electric field the velocity relaxation rate is threefold degenerate. With increasing electric field the smallest eigenvalue, corresponding to particle number (dash-dotted line), exhibits a slight decrease reflecting the increase of the lifetime with the field. Since recombination processes occur practically only from the bottom of the band, their probability is reduced with increasing carrier energy. Therefore, the fraction of free carriers becomes nearly unity and the smallest eigenvalue is only determined by the generation rate. Above a field of about  $25 \text{ kV/cm}$  the recombination rate becomes so small, while at the same time the scattering rate becomes so large that from the MC simulation it is no longer possible to obtain a correlation function for  $u$  within a reasonable CPU time. However, since at these high fields the coupling between the other variables and  $u$  is negligible, it is sufficient to study the system without GR processes.

The other two eigenvalues increase with the field because of the increasing scattering efficiency at higher energies. The energy relaxation rate (dashed line), however, increases much faster than the longitudinal velocity relaxation rate (solid line) due to the onset of optical phonon emission. At some electric field  $E_{crit1} \approx 0.9 \text{ kV/cm}$  these two eigenvalues become equal and, increasing the field strength further, we have now a pair of complex conjugate eigenvalues. In this region velocity and energy relaxation are strongly coupled. A complex eigenvalue always indicates some kind of ordering in the system. In our case it is the joint action of the electric field and the emission of optical phonons. In its extreme case this is well-known as the condition of “streaming motion” [6,7]. When the electric field is increased further, there exists a second critical field  $E_{crit2} \approx 60 \text{ kV/cm}$  above which the eigenvalues again become real. At these very high fields, the dissipation in the system is now so strong that no ordering can be maintained anymore.

Another interesting result is that the relaxation rate of the transverse velocity (dotted line)

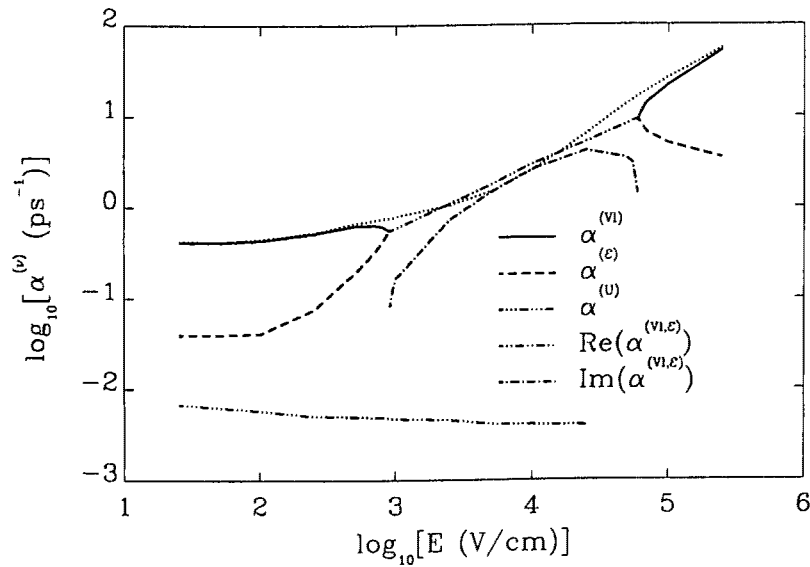


Figure 6: Eigenvalues of the matrix  $\alpha$  as function of the electric field. The solid, dotted, dashed, and dash-dotted lines refer to the eigenvalues corresponding to longitudinal velocity, transverse velocity, energy, and particle number, respectively. In the range between the two critical fields of about  $0.9 \text{ kV/cm}$  and  $60 \text{ kV/cm}$ , due to the large coupling between longitudinal velocity and energy, their corresponding eigenvalues are complex conjugate. There, the solid line refers to the real part and the triple-dot dashed line to the imaginary part.

and the real part of the eigenvalue corresponding to the longitudinal velocity (solid line) are in very good agreement over the whole range of the electric field. This means that these quantities still define a relevant time-scale also for the longitudinal motion of the carrier system.

We remark that at the lowest and highest fields the eigenvalues well agree with the phenomenological rates as well as with the diagonal components of the relaxation matrix.

## 4 Conclusions

We have presented a critical analysis of the relaxation rates describing carrier transport at arbitrary electric field strengths. Three types of rates have been introduced: a phenomenological one, related to the balance equations, and two others which are rigorously derived from the correlation functions. While the former can be appropriately used to describe steady state transport, the rates obtained from the relaxation matrix seem to be more appropriate to analyze a.c. characteristics.

This work has been partially supported by the CEC ESPRIT II BRA 3017 project.

## References

- [1] G. Baccarani, M. Rudan, R. Guerrieri and P. Ciampolini, in "Process and Device Modeling", ed. by W. L. Engl (Elsevier/North-Holland, New York, 1986).
- [2] S. Selberherr, "Analysis and Simulation of Semiconductor Devices" (Springer, Wien-New York, 1984).



- [3] W. Quade and M. Rudan, Proc. of the 19th European Solid State Device Research Conference (ESSDERC 89).
- [4] R. Thoma, A. Emunds, B. Meinerzhagen, H. J. Peifer, and W. L. Engl, IEEE Trans. Electron. Dev., to be published.
- [5] J.P. Nougier, J.C. Vaissiere, D. Gasquet, J. Zimmermann, and E. Constant, J. Appl. Phys. **52**, 825 (1981).
- [6] L. Reggiani, "Hot Electron Transport in Semiconductors", Topics in Applied Physics Vol. 58 (Springer-Verlag, Berlin, Heidelberg, 1985).
- [7] P. Lugli, L. Reggiani and J. J. Niez, Phys. Rev. **B40**, 12382 (1989) .
- [8] T. Kuhn, L. Reggiani, L. Varani, and V. Mitin, Phys. Rev. **B42**, 5702 (1990).
- [9] L. Reggiani, T. Kuhn, L. Varani, D. Gasquet, J.C. Vaissiere, and J.P. Nougier, Proc. ESSDERC 90, editors W. Eccleston and P.J. Rosser, (IOP Publ. Bristol, 1990) p. 489.
- [10] R. Brunetti, and C. Jacoboni, Phys. Rev. **B29**, 5739 (1984).
- [11] T. Kuhn, L. Reggiani, and L. Varani, Phys. Rev. **B42**, 11133 (1990) .